

Strain-induced disorder and phase transformation in hexagonal boron nitride under quasi-homogeneous pressure: *In situ* X-ray study in a rotational diamond anvil cell

V. I. LEVITAS, J. HASHEMI and Y. Z. MA

*Texas Tech University, Center for Mechanochemistry and
Synthesis of New Materials, Department of Mechanical Engineering
Lubbock, TX 79409-1021, USA*

received 26 January 2004; accepted in final form 17 September 2004

published online 29 October 2004

PACS. 64.60.-i – General studies of phase transitions.

PACS. 64.70.Kb – Solid-solid transitions.

Abstract. – One of the challenges in characterization of strain-induced transformations is to create uniform pressure. In this letter, conditions for nearly homogeneous pressure distribution are predicted and achieved experimentally. Compared to hydrostatic loading, plastic shear generally reduces the transformation pressure significantly. We observed, however, an unexpected phenomenon: the transformation of hexagonal to superhard wurtzitic BN under pressure and shear initiated at a pressure comparable to that in hydrostatic compression (~ 10 GPa). *In situ* X-ray diffraction revealed that plastic shear increases the disorder, while hydrostatic compression does not. This increase neutralizes the transition pressure reduction caused by shear. For the same disorder, shear reduced the transformation pressure significantly, and caused a complete, irreversible transformation.

Introduction. – A basic problem in the study and characterization of strain-induced phase transformations under high pressure in a diamond anvil cell is to create a homogeneous stress state across the sample [1–4]. This problem is important not only from a basic research perspective, but also for industrial applications. The transformation of graphite-like hexagonal boron nitride hBN to dense superhard wurtzitic wBN is especially challenging because it is accompanied by a volume reduction factor of 1.53. However, it is of great applicative importance. wBN has wide application due to its hardness and excellent chemical and thermal stability. In industry, wBN is synthesized by explosive loading. Understanding the mechanism of static strain-induced synthesis of wBN at room temperature could lead to a significant technological advance.

We have carried out the first *in situ* X-ray diffraction studies in a rotational diamond anvil. The objectives of our studies were: a) to find theoretically and create experimentally conditions for homogeneous pressure distribution in a sample chamber under compression and shear, before and during phase transformation; b) to study strain-induced disordering and

phase transformation in the hBN using *in situ* synchrotron X-ray diffraction. We succeeded in obtaining an almost homogeneous pressure distribution in both hBN and the resulting wBN by using a gasket with theoretically estimated geometric parameters.

The superposition of large plastic shear on high pressure in a rotational diamond anvil cell dramatically changes the microstructure, thermodynamics, and kinetics of phase transformations [1, 2]. Large plastic shear reduces the transformation pressure by a factor of 2 to 5 for typical materials [1, 2]. We found that hBN transforms into wBN under a hydrostatic pressure of 10.4 GPa; under superimposed shear this transformation occurred at 9.6 GPa. This is nearly the same pressure within experimental uncertainty. We explain this result by noting that the transformation pressure in hexagonal systems is highly correlated with the increase in the degree of three-dimensional disorder characterized by the concentration of turbostratic stacking faults, s . These faults are formed by relative rotations and displacements of two parts of the crystal lattice in (001) planes to arbitrary positions [5–7]. Increase in disorder also slows down kinetics. In particular, in shock experiments at a pressure of $p = 20$ GPa, the volume fraction, c , of wBN grows with decreasing s from $c = 0$ for $s \geq 0.1$ to $c = 0.8$ for $s = 0.03$ [5]. Here, *in situ* X-ray diffraction revealed that plastic shear increases the disorder, while hydrostatic compression does not. This increase in disorder neutralizes the reduction in transition pressure caused by shear.

Experimental methods. – Hexagonal boron nitride was loaded in stainless-steel gaskets and tested in a rotational diamond anvil cell [2] with $500\ \mu\text{m}$ diamond culets (see inset in fig. 1). A two-step loading process was used for both samples: i) compression to some hydrostatic pressure and ii) superposition of plastic shear by controlled rotation of the anvil. The process was repeated at various pressure levels. The thickness, h , of the sample under load was measured using an electric capacity sensor. Pressure distributions were measured using the ruby fluorescence technique. X-ray diffraction was carried out with HZG-4 X-ray diffractometer with Cu K_α radiation (for post loading analysis of some samples) and synchrotron energy dispersive X-ray system at X17C and X17B, National Synchrotron Light Source, Brookhaven National Laboratory (for *in situ* analysis of samples). In addition, two other samples were studied, *in situ*, under hydrostatic conditions.

Conditions for quasi-homogeneous pressure. – The pressure gradient at the interface between the anvil and the sample is caused by the radial component of the frictional stress, τ_r , according to the simplified equilibrium equation $\partial p / \partial r = -2\tau_r / h$ [2, 3]. For an intensive radial flow in a thin disk (under pure compression), τ_r reaches its maximum possible value, $\tau_r = \tau_Y = \sigma_Y / \sqrt{3}$, and thus creates the large pressure gradient observed experimentally [1–4]. Here τ_Y and σ_Y are the yield strengths in shear and compression, respectively.

To achieve high homogeneous pressure one can use a strong gasket that essentially prohibits (limits) radial flow in the specimen. Based on the slip-line solution [8], in the central part of a thin solid cylinder, where $r < h$, a rigid zone appears. In this zone, the corresponding frictional stress is much smaller than τ_Y due to small sliding. Integrating the equilibrium equation for the gasket with an external radius R and internal radius \bar{r} and the boundary condition $p = \sigma_0 + \sigma_Y$ for $r = R$, we obtain

$$\bar{p} = p(\bar{r}) = \sigma_0 + \sigma_Y \left[(1 + 2(R - \bar{r}) / \sqrt{3}h) \right]. \quad (1)$$

Here σ_0 is the lateral pressure at $r = R$. It is clear that the condition $\bar{p} = p_s$ (p_s is the homogeneous pressure inside the specimen), necessary for $\dot{\epsilon} = 0$, cannot be fulfilled during the entire process. We can ensure a decrease in radius \bar{r} if we fulfill the inequality $\bar{p} > p_s$ in all stages of compression and rotation. The decrease in \bar{r} decreases the ratio \bar{r}/h and can only be

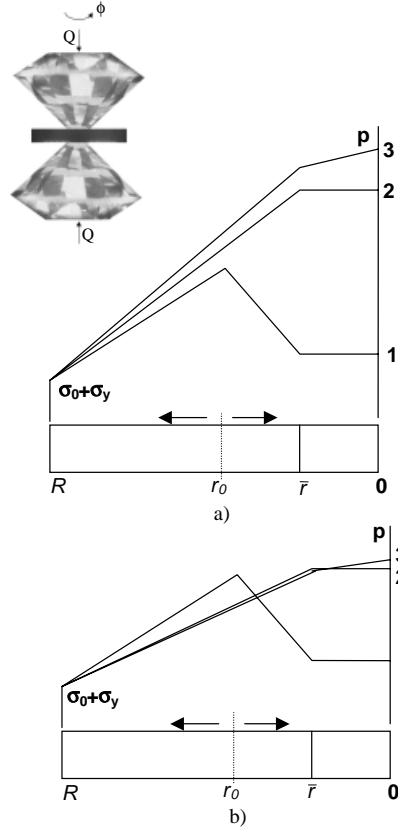


Fig. 1 – Calculated pressure distribution in the sample during (a) compression and (b) rotation under constant load. A schematic of the anvils, gasket, applied load and rotation are shown in the inset. For $\bar{p} > p_s$, material to the right of the neutral radius r_0 moves to the center of the specimen (curve 1), causing change in the sign of frictional stress and pressure gradient. For $\bar{p} < p_s$, plastic flow in the specimen will occur from the center, frictional stress will grow together with pressure gradient in the specimen (curve 3).

due to elastic compression (for void-free material), while an increase in \bar{r} can also be caused by plastic flow and can be much larger. Figure 1 illustrates the importance of the inequality $\bar{p} > p_s$ for homogeneous pressure distribution in the specimen. A simple scheme for the determination of the geometric parameters of the gasket and the specimen is proposed. By measuring two values of the pressure \bar{p} for two different thicknesses when \bar{r} grows (fig. 1a, curve 3), we estimate the parameters σ_0 and σ_Y assuming that they are approximately the same for both h . Let us choose the maximal pressure of interest in the sample p_s and $\bar{r} = h$. Based on the condition $\bar{p} = p_s$, we can then find from eq. (1) the ratio R/h and consequently \bar{r} for maximum load.

Based on the results from the first sample (see below), *i.e.* using $R = 250 \mu\text{m}$, $\bar{r} = 150 \mu\text{m}$, $\bar{p} = 10 \text{ GPa}$ for $h = 58 \mu\text{m}$ and $\bar{p} = 25 \text{ GPa}$ for $h = 11 \mu\text{m}$, we obtained $\sigma_0 = 4.73 \text{ GPa}$ and $\sigma_Y = 1.76 \text{ GPa}$. To achieve a maximum pressure of $p_s = 10 \text{ GPa}$ before transformation, we obtain $R/h = 2.7$ and $h = \bar{r} = 92.5 \mu\text{m}$. Thus, we chose an initial $\bar{r} = 100 \mu\text{m}$ to account for a reduction in \bar{r} due to porosity of hBN in the initial stages of compression. It can be shown that this condition is also sufficient for quasi-homogeneous pressure distribution during the rotation of the anvil under constant force before and in the course of the phase transformation.

TABLE I – The loading history, disorder, and phase fraction data. During a rotation increment, ϕ , pressure varies from the value shown in the previous loading step to the value in the current step. The hyphen indicates measurements at locations other than center, within the same loading step. The asterisk indicates no pressure measurements were performed at that point.

| Loading step | p (GPa) | ϕ° | r (μm) | β° | s | c |
|--------------|--------------|--------------|--------------------------|---------------|-------|------|
| 1 | 0 | 0 | 0 | 0.299 | 0.077 | 0.0 |
| 2 | 2.1 | 0 | 0 | 0.330 | 0.085 | 0.0 |
| 3 | 3.8 | 0 | 0 | 0.367 | 0.095 | 0.0 |
| – | 4.2 | 0 | 40 | 0.349 | 0.091 | 0.0 |
| 4 | * | 20 | 0 | 0.315 | 0.082 | 0.0 |
| 5 | 3.8 | 50 | 0 | 0.362 | 0.094 | 0.0 |
| 6 | 6.4 | 0 | 0 | 0.374 | 0.098 | 0.0 |
| 7 | * | 20 | 0 | 0.394 | 0.103 | 0.0 |
| 8 | 5.8 | 70 | 0 | 0.491 | 0.127 | 0.0 |
| – | 6.6 | 0 | 30 | 0.408 | 0.106 | 0.0 |
| 9 | 9.6 | 0 | 0 | 0.405 | 0.107 | 0.05 |
| 10 | * | 25 | 0 | 1.107 | 0.267 | 0.70 |
| – | * | 0 | 40 | 0.968 | 0.238 | 0.63 |
| 11 | 10.3 | 70 | 0 | 1.176 | 0.278 | 0.64 |
| 12 | 10.6 | 205 | 0 | | | 1.0 |
| 13 | 13.9 | 0 | 0 | | | |
| 14 | * | 30 | 0 | | | |
| 15 | 25.2 | 30 | 0 | | | |

Experimental results and discussion.

First sample. A gasket with an initial hole radius of $\bar{r} = 125 \mu\text{m}$ and thickness $h = 212 \mu\text{m}$ was used. After compression to 5 GPa, the hole containing hBN began to grow. At 10 GPa and $h = 58 \mu\text{m}$, a rotation $\phi = 120^\circ$ led to $h \approx 24 \mu\text{m}$ at $\bar{r} \approx \text{const}$. At $p = 25$ GPa, $h = 11 \mu\text{m}$, additional rotation $\phi = 240^\circ$ led to $h = 5 \mu\text{m}$. X-ray diffraction measurements indicated that all patterns for different positions along the radial direction were identical and could be indexed into wBN. We noticed that the weak and broad peak at 0.21 nm may possibly be an overlap of cBN (111) and wBN (002) peaks. Yet, no other indications for cBN exist. Thus we believe that a complete hBN \rightarrow wBN transformation has occurred. The results from this measurement were used to determine the parameters σ_0 and σ_Y and the geometric parameters of the gasket to create a homogeneous pressure in the sample.

Second sample. A gasket with initial hole radius $\bar{r} = 100 \mu\text{m}$ and $h = 212 \mu\text{m}$ was used. A thin layer of ruby grains ($< 0.5 \mu\text{m}$) was placed on one side of the hBN sample to measure the pressure distribution. The loading program is presented in table I. Figure 2 demonstrates success in achieving an almost homogeneous pressure distribution in all stages of compression up to 10 GPa. The rotation of the anvil (before phase transformation) neither introduced significant pressure inhomogeneity nor led to an appreciable pressure increase. At 9.6 GPa and $\phi = 95^\circ$ (fig. 2f), the pressure at the periphery of the sample increased by 2 GPa during hBN \rightarrow wBN transformation (the pressure at the center was unchanged). The pressure growth indicates that the volume reduction, due to transformation, is offset by the reduction in thickness due to rotation. At this point, the higher elastic properties of wBN cause a slight pressure growth. This indicates that phase transformation is more intensive in the external part of the sample (where plastic shear is maximal). Additional rotation

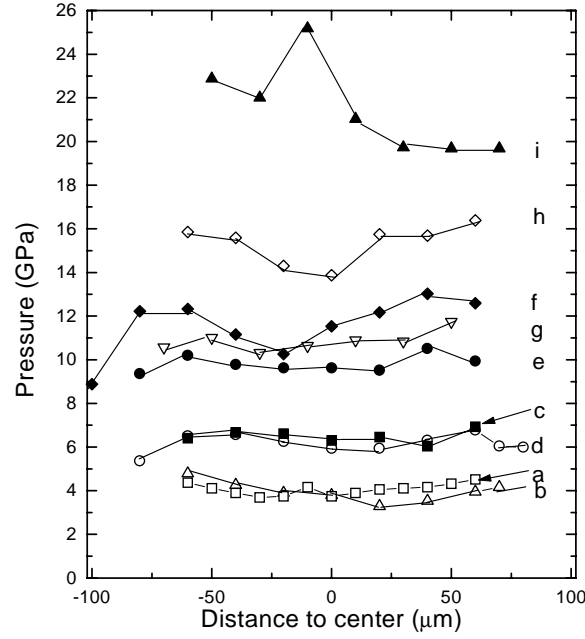


Fig. 2 – Pressure distribution along the radial direction of the sample chamber. a: pressure increase (PI); b: rotation, $\phi = 70^\circ$; c: PI; d: $\phi = 90^\circ$; e: PI; f: $\phi = 95^\circ$; g: $\phi = 205^\circ$; h: PI; i: $\phi = 60^\circ$. The measurement at $100\ \mu\text{m}$ on curve f (8.8 GPa) is at the distorted edge of gasket.

of $\phi = 205^\circ$ completes the transformation throughout the specimen, reduces pressure at the periphery, and ends with a practically homogeneous pressure of 10.6 GPa (fig. 2g). Comparing the pressure distribution before rotation and after the complete transformation, we conclude that a *homogeneous pressure self-multiplication effect* was observed for the first time. After a rotation of $\phi = 60^\circ$, pressures of 20 GPa at the periphery and 25 GPa at the center were recorded. The reason for the pressure increase is the reduction in the thickness of the sample during the rotation of the anvil. The reduction in thickness under a fixed force leads to an increase in pressure in the phase with the higher elastic and plastic properties.

The changes in turbostratic faults and wBN concentrations are presented in table I. The volume fraction of wBN was approximated from [7] using the relationships $c = 45.009x^3 + 18.737x^2 + 34.872x$, and $1 - c = 57.269y^3 - 162.26y^2 + 205.72y$, where $x = I_{110}^w / (I_{110}^w + I_{110}^h)$, $y = I_{110}^h / (I_{110}^w + I_{110}^h)$, and I_{ijk} is the integral intensity of ijk diffraction lines of wBN (superscript w) and hBN (superscript h). The degree of disorder, s , was determined using the relationship for relative broadening $\beta = B_{hkl} - B_{hko}^2 / B_{hkl} = C d_{hko}^2 (s / \sqrt{1 - s}) \tan \theta$, where B_{hkl} (degrees) is the width of hkl diffraction lines, d_{hko} (nm) is the interplanar spacing, θ is the Bragg angle, and $C = 328.8\ (^{\circ}/\text{nm}^2)$ for hBN [5–7,9]. The (110) and (112) planes were used to determine s . While the equations in [6] are based on the angle dispersive approach, we assume that their application for the energy dispersive method will serve as a first approximation of s .

The X-ray diffraction patterns are shown in fig. 3. As a reference, data obtained for the hydrostatic loading case showed that up to 9.4 GPa, changes in s were negligible. This indicates that the disordering of material is induced by plastic strain. In our hydrostatic experiments, the pressure required for initiation of hBN \rightarrow wBN transformation was 10.4 GPa at $s = 0.04$. In comparison, for $s = 0.02 \pm 0.02$, the transformation pressure was 8.2 ± 0.1 GPa [10], which

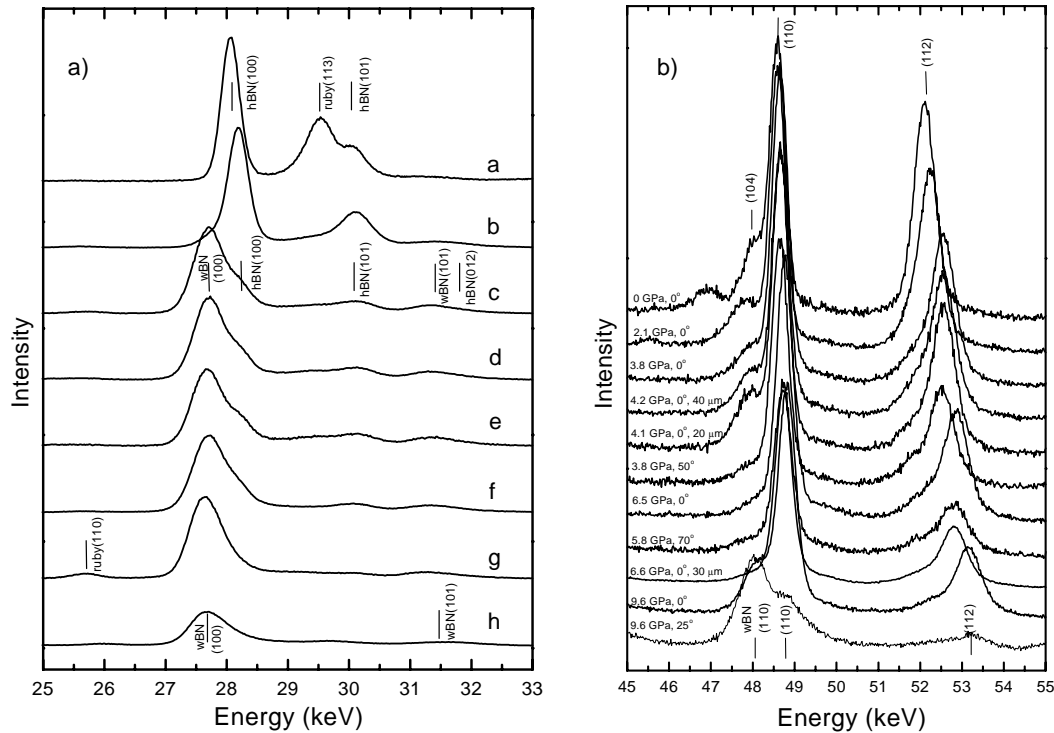


Fig. 3 – a) Comparison of X-ray diffraction patterns of boron nitride during compression and shear loading stages. a: $p = 0$, $\phi = 0^\circ$; b: $p = 9.6$, $\phi = 0^\circ$ ($c = 0.05$); c: $\phi = 25^\circ$ after conditions described by b at $r = 0$ ($c = 0.70$); d: same as c, $r = 20 \mu\text{m}$; e: same as c, $r = 40 \mu\text{m}$; f: $\phi = 70^\circ$ after c, $r = 0$; g: $\phi = 205^\circ$, $r = 0$. b) The progression of broadening of (110) and (112) peaks of boron nitride during compression and shear loading stages; X-ray measurements were performed at the center of the sample, except those marked with μm values indicating distance from center.

is consistent with the tendency that an increase in s increases the transformation pressure. Under plastic compression up to 9.6 GPa and rotation up to 160° , s grows from 0.077 to 0.106–0.127. This has to increase the hBN \rightarrow wBN phase transformation pressure significantly. However, the first traces of wBN, $c = 0.05$, were observed after compression of up to 9.6 GPa. The results indicate that phase transformation may be caused by large rotations of the anvil, even under lower pressures. A volume fraction $c = 0.70$ was reached at $\phi = 25^\circ$ in a pressure range of 9.6–10.3 GPa, along with an increase in s to 0.238–0.267. Because of the appearance of strong wBN particles, plastic strain in weak hBN is much larger than that prescribed for the specimen. Also, hBN \rightarrow wBN phase transformation occurs predominantly in the well-ordered regions of hBN crystal lattice. This must increase s even without further strain-induced disordering. This is consistent with the fact that a small increase in s is introduced under an additional $\phi = 70^\circ$ when phase transformation is also arrested due to high s .

After unloading of both specimens, scratches and particles of sizes up to a few microns were found on the diamond anvil surface. The particles could not be removed by the mechanical means we applied. Both Raman and synchrotron X-ray techniques yielded inconclusive results. We have not yet ruled out the possibility of the formation of a new phase under our experimental conditions.

Concluding remarks. – In this letter, conditions for nearly homogeneous pressure distribution for a sample under pressure and shear were predicted and achieved experimentally. This allowed us to quantitatively study the strain-induced transformation in hBN. Plastic straining causes two conflicting processes that determine the thermodynamics and kinetics of phase transformation. First, plastic straining produces new defects (stress concentrators), which serve as a nucleation site, thus promoting phase transformation. Second, in hexagonal systems, plastic strain increases the disorder s that, in turn, suppresses the martensitic phase transformation. As a result, hBN \rightarrow wBN phase transformation was initiated at a pressure of 9.62 GPa under compression; the yield increased to $c = 0.70$ at $\phi = 25^\circ$ and 9.6–10.3 GPa; completed at $\phi = 205^\circ$ and 10.6 GPa. This phase transformation pressure is much lower and the phase transformation progress is much more intensive than in known data for similar values of s [5]; it is also irreversible.

* * *

Thanks are due to Drs. H.-K. MAO, J. Z. HU, and Q. Z. GUO for supporting this research with synchrotron X-ray diffraction. Assistance by Dr. M. HOLTZ and N. GUVEN is also appreciated. Support of the Texas Tech Excellence Fund is gratefully acknowledged.

REFERENCES

- [1] BLANK V. *et al.*, *Sov. Phys. JETP*, **87** (1984) 922; ALEKSANDROVA M. *et al.*, *Solid State Phys.*, **29** (1987) 2573; **35** (1993) 1308; SEREBRYANAYA N. R. *et al.*, *Phys. Lett. A*, **197** (1995) 63; BLANK V. *et al.*, *Phys. Lett. A*, **188** (1994) 281; BLANK V. D. and BUGA S. G., *Instrum. Exper. Techn.*, **36** (1993) 149.
- [2] NOVIKOV N., POLOTNYAK S., SHVEDOV L. and LEVITAS V., *J. Superhard Mater.*, **3** (1999) 39.
- [3] LEVITAS V. I., *J. Mech. Phys. Solids*, **45** (1997) 923; 1203.
- [4] LEVITAS V. I. and SHVEDOV L., *Phys. Rev. B*, **65** (2002) 104109.
- [5] BRITUN V. F. and KURDYUMOV A. V., *High Pressure Res.*, **17** (2000) 101.
- [6] KURDYUMOV A. V., *Sov. Phys. Crystallogr.*, **20** (1975) 969.
- [7] KURDYUMOV A. V., MALOGOLOVETZ V. G., NOVIKOV N. V. *et al.*, *Polymorphic Modifications of Carbon and Boron Nitride* (Metallurgy, Moscow) 1994.
- [8] LEVITAS V. I., *Large Deformation of Materials with Complex Rheological Properties at Normal and High Pressure* (Nova Science Publishers, New York) 1996.
- [9] PETRUSHA I., private communications.
- [10] SOLOZHENKO V. L. and ELF F., *J. Superhard Mater.*, **3** (1998) 67.